Severe Drought Conditions in Northern East Asia During the Early Pliocene Caused by Weakened Pacific Meridional Temperature Gradient

Yanhong Zheng, Alexey V. Fedorov, Natalie J. Burls, Rui Zhang, Chris M. Brierley, Zhengkun Fang, Xuefeng Yu, Feng Xian, Hongxuan Lu

Geophysical Research Letters

RESEARCH LETTER
10.1029/2022GL098813

Key Points:

- Severe drought conditions persisted throughout the early Pliocene epoch over Northern China
- We link these conditions to the reduced meridional temperature gradient in the Pacific Ocean
- The reduced Pacific meridional temperature gradient acts to weaken the summer East Asian monsoon precipitation over Northern China

Supporting Information:

Supporting Information may be found in the online version of this article.

Correspondence to:

Y. Zheng and A. V. Fedorov,
zhengnwu@163.com;
alexey.fedorov@yale.edu

Citation:

Zheng, Y., Fedorov, A. V., Burls, N. J., Zhang, R., Brierley, C. M., Fang, Z., et al. (2022). Severe drought conditions in northern East Asia during the early Pliocene caused by weakened Pacific meridional temperature gradient. *Geophysical Research Letters*, *49*, e2022GL098813. https://doi.org/10.1029/2022GL098813

Received 22 MAR 2022
Accepted 1 JUL 2022

Author Contributions:

Conceptualization: Yanhong Zheng, Alexey V. Fedorov
Formal analysis: Yanhong Zheng, Natalie J. Burls, Chris M. Brierley, Zhengkun Fang, Hongxuan Lu
Funding acquisition: Yanhong Zheng
Investigation: Yanhong Zheng, Rui Zhang, Zhengkun Fang, Xuefeng Yu, Feng Xian
Methodology: Yanhong Zheng, Alexey V. Fedorov, Natalie J. Burls, Chris M. Brierley
Project Administration: Yanhong Zheng
Resources: Yanhong Zheng, Rui Zhang
Software: Natalie J. Burls, Chris M. Brierley
Supervision: Yanhong Zheng, Alexey V. Fedorov
Validation: Yanhong Zheng

Severe Drought Conditions in Northern East Asia During the Early Pliocene Caused by Weakened Pacific Meridional Temperature Gradient

Yanhong Zheng[1,2], Alexey V. Fedorov[3,4], Natalie J. Burls[5], Rui Zhang[1], Chris M. Brierley[6], Zhengkun Fang[1], Xuefeng Yu[2], Feng Xian[2], and Hongxuan Lu[2]

[1]State Key Laboratory of Continental Dynamics, Department of Geology, Northwest University, Xi'an, P. R. China, [2]State Key Laboratory of Loess and Quaternary Geology, Institute of Earth Environment, Chinese Academy of Sciences, Xi'an, P. R. China, [3]Department of Earth and Planetary Sciences, Yale University, New Haven, CT, USA, [4]LOCEAN/IPSL, Sorbonne University, Paris, France, [5]Department of Atmospheric, Oceanic & Earth Sciences, Center for Ocean-Land-Atmosphere Studies, George Mason University, Fairfax, VA, USA, [6]Department of Geography, University College London, London, UK

Abstract The evolution of hydroclimate in East Asia during the Pliocene—a potential analog of the future greenhouse climate—remains highly uncertain. Here we reconstruct changes in the hydroclimate of Northern China during this epoch. Our results reveal previously undocumented severe drought conditions that persisted through the early Pliocene with a significantly greater magnitude than suggested by other records. Using a broad hierarchy of climate simulations, we find that reduction in the Pacific meridional sea surface temperature (SST) gradient has particularly strong impacts on precipitation over Northern China, which suggests its key role in maintaining drought conditions during the early Pliocene. The weaker Pacific meridional SST gradient causes the weakening of the East Asian summer monsoon precipitation over this region via a reduction of atmospheric northward moisture transport from the ocean, which enhances aridity inland. Our results highlight the fundamental control of the tropical ocean on the extra-tropical hydrological cycle.

Plain Language Summary Understanding East Asian rainfall changes with global warming is an important issue of climate sciences. The Pliocene epoch provides a potential analog to the future greenhouse climate. Here, for the first time we reconstruct high-resolution aridity changes over the Chinese Loess Plateau (CLP) in northern East Asia during the Pliocene. Our results indicate persistent drought conditions over CLP during the early Pliocene. Analyzing a broad range of climate model simulations, we find that the reduced meridional sea surface temperature gradient is a critical factor in the weakening of the East Asian summer monsoon over Northern China and in maintaining drought conditions during the early Pliocene relative to the late Pliocene. Our results expand the Asian inland paleoclimate records during the Pliocene, providing new information on past Asian monsoon precipitation variations during the warm Pliocene with potential implications for future hydroclimate changes under greenhouse warming in East Asia.

1. Introduction

The Asian monsoon system plays a key role in the climate system and influences societal and economic development over East Asia. Understanding East Asian rainfall changes on geological timescales is a critical issue of climate science, in particular during the Pliocene epoch (Feng et al., 2022; Han et al., 2021). This epoch is characterized by atmospheric CO_2 levels similar or slightly higher than the present anthropogenically elevated levels (Fedorov et al., 2013; Foster et al., 2017; Robinson et al., 2008), and global mean temperatures 2–5°C warmer than the preindustrial (Brierley & Fedorov, 2010; Dowsett et al., 2012; Haywood et al., 2013, 2020), which resembles climate scenarios that may become possible during the 21st century (Burke et al., 2018).

Long-term changes in East Asian paleoclimate have been widely investigated; however, existing hydroclimate reconstructions disagree on trends during the Pliocene Epoch, as there exist large uncertainties in the estimated variations of summer monsoon precipitation in Northern China during the early Pliocene (An et al., 2005; Nie et al., 2014; Qin et al., 2022; Sun et al., 2010; H. L. Wang et al., 2019). Thus, East Asian hydroclimate is still not fully understood. In particular, little is known about drought conditions in East Asia during this period.

Visualization: Yanhong Zheng, Alexey V. Fedorov, Xuefeng Yu, Feng Xian
Writing – original draft: Yanhong Zheng
Writing – review & editing: Yanhong Zheng, Alexey V. Fedorov, Natalie J. Burls

Several possible mechanisms have been proposed to explain Asian monsoon rainfall variations during the Pliocene, including the uplift of the Tibetan Plateau (An et al., 2001), remote effects of the gradual closure of the Central American Seaway (Nie et al., 2014), global cooling (H. L. Wang et al., 2019), the combined effect of high- and low-latitude insolation forcings (Y. Wang et al., 2020), and vegetation and ice sheet changes (Feng et al., 2022). In addition, it has been suggested that the reduction of large-scale meridional and zonal sea surface temperature (SST) gradients strongly impacted the hydrological cycle of the Northern Hemisphere (Burls & Fedorov, 2017; J. Lu et al., 2021). Accordingly, the goal of this paper is to reconstruct Pliocene aridity changes based on glycerol dialkyl glycerol tetraethers (GDGTs) in the Shilou red-clay sequence on the Chinese Loess Plateau (CLP) in Northern China (Figure 1), and to explore the physical factors that may have controlled those aridity changes using climate model simulations, focusing on the role of changes in meridional and zonal SST gradients in the Pacific Ocean.

GDGTs are produced by archaea and bacteria living in soils—and have been previously applied to reconstruct paleoclimate conditions (H. X. Lu et al., 2019; Peterse et al., 2014). In general, wet acidic conditions in soils are favorable for the branched (br) GDGT producing bacteria, whereas archaea (e.g., Thaumarchaea) producing the isoprenoid (iso) GDGTs grows well in dry alkaline soils (Dirghangi et al., 2013; Weijers et al., 2006). Consequently, the abundance of archaeal isoGDGTs (bacterial brGDGTs) is higher (lower) in dry alkaline soils than in wet acid soils, and vice versa (Xie et al., 2012; Yang et al., 2014). Especially, the abundance of archaeal isoGDGTs relative to bacterial brGDGTs ($R_{i/b}$) increases substantially in extremely arid conditions, and thus has been considered a reliable indicator of enhanced drought conditions in terrestrial archives (Tang et al., 2017; Xie et al., 2012). In addition, the Branched and Isoprenoid Tetraethers (BIT) index provides an estimate of the relative abundance of bacterial GDGTs and crenarchaeol which is only synthesized by Thaumarchaeota. This index is related to mean annual precipitation (MAP) (Dirghangi et al., 2013) and water content (H. Wang et al., 2013) in soils. It has been suggested as another hydrological proxy with lower values indicating dry conditions (Tang et al., 2017; Yang et al., 2014). Although the BIT index is not as robust as $R_{i/b}$ in some settings, such as extremely alkaline deposits (Yang et al., 2014), the two indices analyzed together have a strong tandem utility as hydrological proxies in soils.

Here, for the first time we apply these two novel proxies, combined with a broad range of model simulations, to explore monsoon-driven aridity changes on the CLP during the Pliocene and examine the causes of these variations focusing on persistent drought conditions during the early Pliocene. Our results expand the Asian inland paleoclimate records for the period between ca. 2.5–5.2 Ma, thus providing critical new information on Asian monsoon precipitation variations during the Pliocene with potential implications for future hydroclimate changes under greenhouse warming in East Asia.

2. Materials and Methods

2.1. Data

The Shilou red clay sequence is located at the eastern edge of the CLP (Figure 1). This aeolian profile contains 2.8 m of Quaternary loess-paleosol sequence and 69.2 m of red-clay sequence. The new magnetostratigraphy provides a well-constrained age model of 5.2 Ma for the Shilou Red Clay sequence (Anwar et al., 2015). The homogenized materials (~25 g) were extracted with dichloromethane: methanol (9:1) using an accelerated solvent extractor at 100°C and 1500 psi. The procedures for lipid extraction and analysis, the $R_{i/b}$ and BIT proxies are further described in Supporting Information S1.

2.2. Modeling

Complementary climate model simulations have been analyzed to investigate the effects of meridional and zonal SST gradients on aridity over the CLP and confirm our data-based inferences. We use two sets of experiments with general circulation model (GCMs), in which anomalous precipitation minus evaporation (P-E) serves as a measure of aridity. The first set of experiments involves predominantly coupled ocean-atmosphere GCM experiments wherein the zonal and meridional SST gradients vary together. We have performed a large number of integrations to simulate different climate states characterized by distinct cloud albedo perturbations (induced by cloud water path modifications over latitudinal bands, Figure S2 in Supporting Information S1) or different CO_2 increases, and correlate P-E anomalies over the CLP with the simulated meridional and zonal SST gradients.

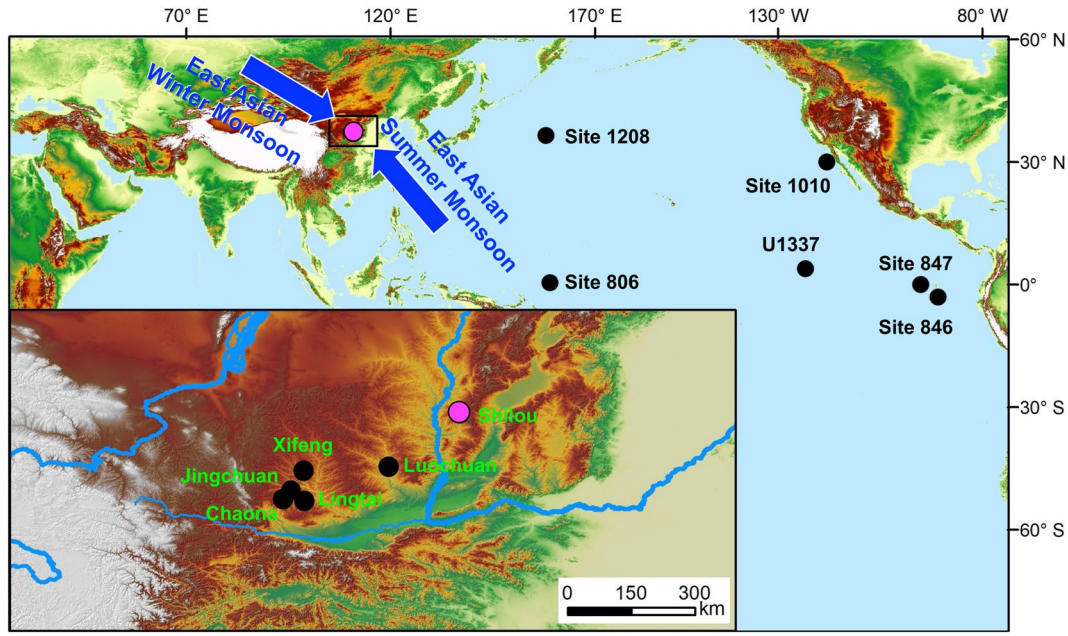

Figure 1. Topography of East Asia, the location of Shilou and other sites on the Chinese Loess Plateau, and the relevant ocean sites with proxy sea surface temperature data. The arrows show approximate wind direction of the East Asian monsoon in summer and winter.

The second set of experiments uses an atmosphere-only GCM wherein we can modify the meridional and zonal SST gradients separately, in order to isolate their effects on P-E over East Asia. Further details on the design of these two sets and the GCMs used are provided in Supporting Information S1.

3. Results

3.1. Drought Conditions Over the CLP During the Early Pliocene

The $R_{i/b}$ ratio and BIT index in the Shilou Red-clay sequence vary from 0.04 to 3.8 and from 0.3 to 0.97, respectively, during the Pliocene interval 5.2–2.5 Ma. Both indices exhibit similar trends throughout the whole sequence (Figures 2c and 2d). High $R_{i/b}$ ratios and low BIT values are observed with large fluctuations between ca. 5.2 and 4.0 Ma. Specifically, the records reveal dramatic increases in $R_{i/b}$ ratios and decreases in BIT values around 5.2–5.1, 5.0–4.8, 4.7, 4.5, 4.3, and 4.1 Ma. During the early Pliocene from ca. 5.2 to 4.0 Ma, most values of $R_{i/b}$ ratios are higher than 0.5, which is much higher than those during the late Pliocene and very early Pleistocene from ca. 4.0 to 2.5 Ma (Figures 2c and 2d).

Modern evidence shows that the $R_{i/b}$ ratios remain low (<0.5) and stable when precipitation is >600 mm in soils, whereas the $R_{i/b}$ ratios are >0.5 in extreme dry soils on CLP (Xie et al., 2012; Yang et al., 2014). Consequently, high $R_{i/b}$ ratios (>0.5) only record the most severe drought events rather than more subtle or regular drought events (Tang et al., 2017; Xie et al., 2012; Yang et al., 2014). Therefore, during the early Pliocene the elevated $R_{i/b}$ values (>0.5) clearly indicate persistent drought conditions in Shilou region. Additionally, the BIT indices, representing microorganisms different from $R_{i/b}$, exhibit the same trend as the $R_{i/b}$ ratios throughout the Pliocene. Thus, both $R_{i/b}$ and BIT reflect greater aridity in the early Pliocene relative to the mid to late Pliocene.

The extreme drought conditions inferred from the $R_{i/b}$ and BIT ratios in the early Pliocene coincide with a weakened summer monsoon over the region suggested by high coarse grain size content and low magnetic susceptibility of red-clay in Shilou (Figures 2a–2d). Likewise, this much drier climate is broadly consistent with weaker summer monsoon precipitation recorded in other red-clay sequences over the CLP such as Jingchuan, Lingtai and Xifeng (An et al., 2001; Ding et al., 2001; Sun et al., 2010).

Nevertheless, some other paleorecords contradict our records. Specifically, the drier conditions over the CLP during the early Pliocene are not agreement with higher precipitation inferred from the phytolith assemblages

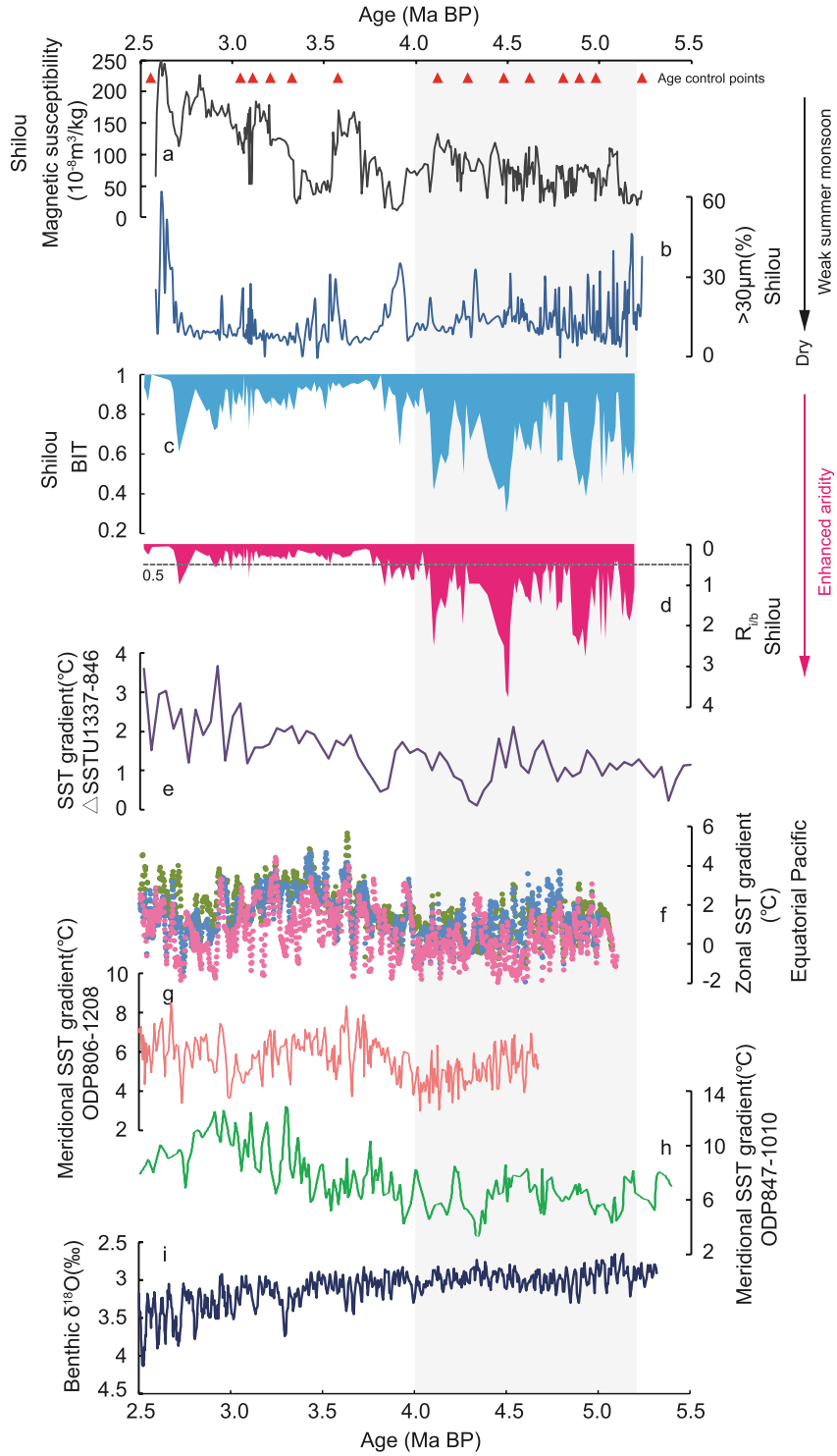

Figure 2. Comparison of the $R_{i/b}$ and Branched and Isoprenoid Tetraethers (BIT) proxies with other records from the Chinese Loess Plateau and the Pacific Ocean. (a) Magnetic susceptibility and (b) Coarse fraction (>30 μm) content in Shilou (Anwar et al., 2015). (c) BIT and (d) $R_{i/b}$ indices in Shilou (this study). (e) The zonal sea surface temperature (SST) gradient between sites U1337 and 846 (Liu et al., 2019). (f) The zonal SST gradient along the equatorial Pacific (806 Mg/Ca–847 Mg/Ca (reddish pink), 806 Mg/Ca–846 alkenones (green), 806 Mg/Ca–847 alkenones (blue); Fedorov et al., 2013 and references therein). (g and h) The meridional SST gradients between sites 806 and 1208, and between sites 847 and 1010 (LaRiviere et al., 2012; Pagani et al., 2010; Wara et al., 2005). (i) Benthic foraminiferal $\delta^{18}O$ record (Lisiecki & Raymo, 2005). The gray shading indicates the high aridity period.

in Lantian on the southeastern margin of the CLP (H. L. Wang et al., 2019). However, phytolith records reflect a complex response of plants to changes in precipitation, evaporation, and temperature, in addition to transport variability, which might complicate the inferred precipitation signal. In contrast, grass-dominated ecosystems in the early Pliocene (H. L. Wang et al., 2019) still suggest a relatively dry climate in comparison with modern, tree-dominated vegetation in Northern China, supporting our conclusions.

We also note that the grain size and magnetic susceptibility records do not necessarily capture the full severity of the drought conditions (Tang et al., 2017), presumably because these records are affected by other variables in addition to precipitation, such as wind intensity, which might dilute the signal. A reduced MAP reconstructed by Nie et al. (2014) from soil magnetic parameters was observed in the early Pliocene on the southern CLP. It is noted that high MAP occurred in some intervals of the early Pliocene where the $R_{i/b}$ values are higher than 0.5. This inconsistency arises because soil magnetic parameters can also correlate with temperature (Nie et al., 2014); and in this case, high temperatures in early Pliocene may lead to an overestimation of MAP. Furthermore, soil magnetic parameters are not sensitive to precipitation when MAP is less than 500 mm, thus potentially causing uncertainties of the reconstructed MAP (Nie et al., 2014).

Overall, the majority of records agree on dry conditions over the CLP in the early Pliocene, but the inferred severity of drought conditions based on our data appears to be much greater than that inferred from both grain size and magnetic records. The anomalously high values of the $R_{i/b}$ ratios and BIT indices provide a strong indication of such extreme drought conditions.

3.2. Topographic Changes Are Unlikely to Cause Early Pliocene CLP Aridity Changes

Topographic changes are often considered a major control of precipitation on geological timescales. East Asian winter and summer monsoons could have been strengthened by the uplift of the Tibetan Plateau (An et al., 2001); however, there is no strong evidence for a significant uplift of the Tibetan Plateau in the early Pliocene. An uplift of the entire Tibetan Plateau might have occurred at around 3.6 Ma (An et al., 2001), potentially enhancing aridity in East Asia via strong winter monsoon (Figure 2b). However, the $R_{i/b}$ (BIT) ratios do not show elevated (low) values at 3.6 Ma.

In addition, the expansion of North Hemisphere ice sheets did not start until around 2.8 Ma (Haug et al., 2005). The small ice sheets could maintain only a relatively weak meridional thermal gradient and thus weak westerlies. These relatively weak westerlies probably carried less dry air masses to the CLP in the early Pliocene. Thus, the Tibetan Plateau uplift and changes in the Northern Hemisphere ice sheets do not appear as plausible explanations for the persistent drought conditions during the early Pliocene on the CLP.

3.3. Dynamical Causes of Severe Drought Conditions During the Early Pliocene

We find that the early Pliocene drought conditions coincide with the occurrence of weakened zonal and meridional large-scale SST gradients in the Pacific Ocean (Figures 2c–2h). Although their exact magnitudes are debated (Tierney et al., 2019), the early Pliocene zonal and meridional SST gradients were substantially weaker (Fedorov et al., 2013, 2015; Liu et al., 2019; Wara et al., 2005). Climate conditions with a reduced zonal SST gradient and a deeper/warmer equatorial thermocline (Ford et al., 2015) are sometimes referred to as a "permanent El Niño-like" state (Fedorov et al., 2010, 2013; Shankle et al., 2021; Wara et al., 2005; White & Ravelo, 2020), invoking an analogy to modern El Niño conditions. In the modern climate, El Niño causes decreased monsoon precipitation over North China due to the weak/southward shift of the West Pacific subtropical High, leading to droughts on the CLP (Huang & Wu, 1989). For example, during the 1997/1998 El Niño event, annual precipitation decreased in the Shilou region more than in any other year of the past 60 years.

Thus, a question arises on the potential role of reduced meridional and zonal SST gradients in the Pacific in maintaining the early Pliocene drought conditions over the CLP. To address this, we use a suite of numerical simulations with a coupled GCM wherein we are able to change these SST gradients in a broad range and investigate the impacts of these gradients on P-E. Our simulations show that, although there is a significant spread between the models, the P-E field over the CLP is well correlated with the zonal SST gradient along the equator ($r = 0.62$; Figure 3b), with smaller P-E values corresponding to a weaker gradient. Yet, we find that the correlation between

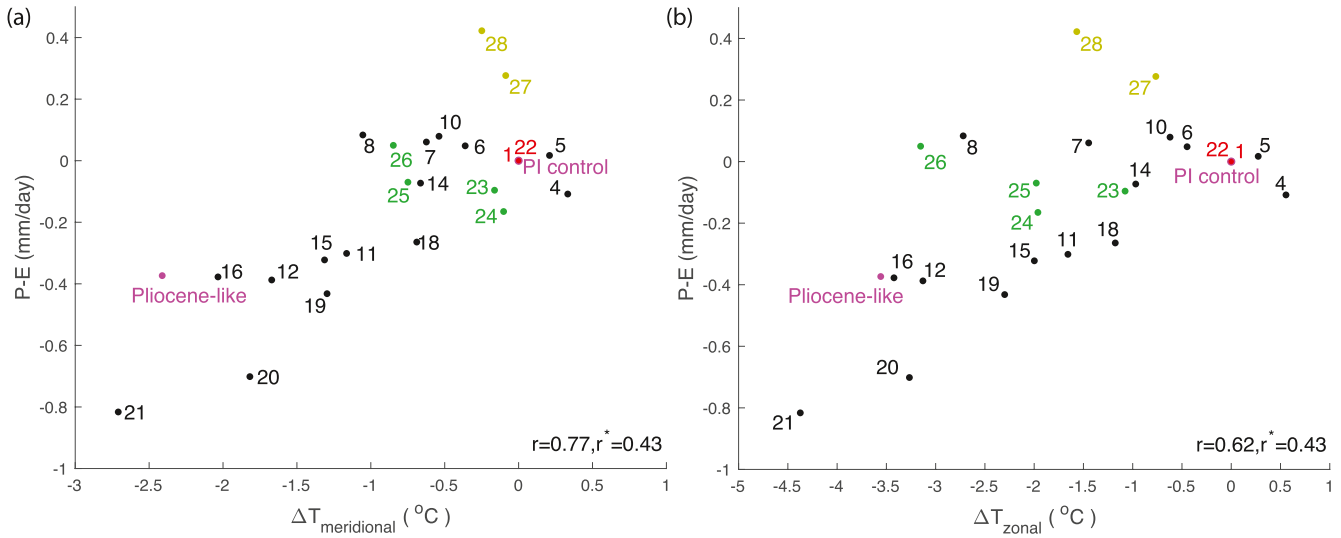

Figure 3. The P-E change relative to the preindustrial control simulation averaged over the Chinese Loess Plateau (34–38°N and 105–115°E) across a suite of climate simulations. P-E is plotted (a) against the meridional sea surface temperature (SST) gradient and (b) the equatorial Pacific zonal SST gradient (see Methods for the gradient definitions). Each dot corresponds to one model climate state simulation and the numbers correspond to those assigned in Burls and Fedorov (2017), with red representing the preindustrial control experiments, black/green—low/high resolution modified cloud forcing experiments, yellow—abrupt CO_2-increase experiments, and purple—prescribed SST experiments. P-E is given in millimeters per day (mm/day). *r* indicates the correlation between variables; *r** is the required correlation value for significance at the 95% level taking into account the effective degrees of freedom.

the meridional SST gradient in the Northern Hemisphere and P-E over the CLP is much stronger (r = 0.77; Figure 3a).

Our synthetic times series of reconstructed P-E since the early Pliocene also show that the meridional SST gradient causes larger P-E changes than the zonal SST gradient (Figure 4). Regardless of the SST gradient reconstruction used, changes in the meridional SST gradient dominate P-E changes, and estimated P-E anomalies indicate higher aridity during the early Pliocene (Figure 4). While the zonal SST gradient is tightly linked to the meridional SST gradient (Burls & Fedorov, 2014; Fedorov et al., 2015), it is the latter that is particularly important for northward heat and moisture transports (Brierley & Fedorov, 2010; Burls & Fedorov, 2017).

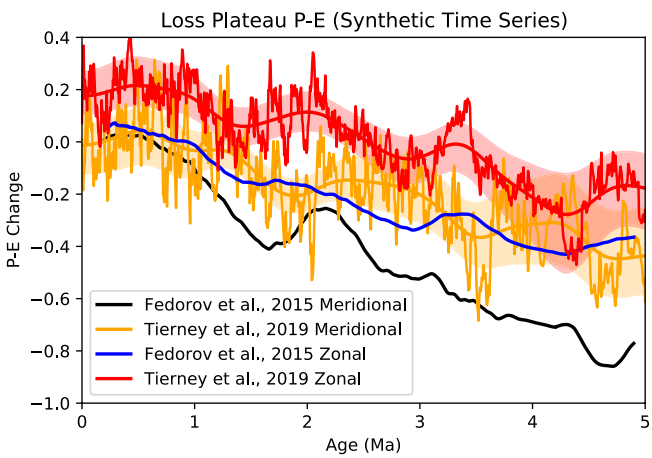

Figure 4. Synthetic time series for Chinese Loess Plateau (CLP) P-E anomalies (in mm/day relative to late Pleistocene/preindustrial) estimated from the zonal and meridional sea surface temperature (SST) gradients reconstructed from multiple records in two different studies (Fedorov et al., 2015; Tierney et al., 2019). These time series are based on simple linear regressions of the simulated relationships between CLP P-E and the meridional and zonal gradients (in Figure 3) that allow for converting reconstructed variations in zonal and meridional SST gradients into P-E anomalies. The light color shading represents the uncertainty range provided for the Tierney et al. (2019) gradient reconstructions.

These results suggest that the meridional SST gradient played a critical role in amplifying drought conditions over Northern China. To further explore the influence of the meridional versus zonal SST gradient we examine two sensitivity experiments in which the zonal SST gradient, and then the meridional SST gradient, is reduced independently following the approach of Brierley & Fedorov, 2010. The results show that the zonal SST gradient reduction leads to reduced precipitation over the CLP in winter rather than summer (Figures 5c and 5d), consistent with previous observations (Dai & Wigley, 2000). Consequently, the zonal gradient can still affect the mean precipitation but to a lesser extent.

A moisture budget analysis shows that changes in the winds caused by the reduced meridional gradient tend to increase precipitation in Southern China but decrease in Northern China (Figure S3b in Supporting Information S1). This tendency is opposite for the reduced zonal gradient (Figure S3e in Supporting Information S1). In the former case, changes in specific humidity also act to reduce precipitation over Northern China (Figure S3c in Supporting Information S1). Thus, the reduction of the meridional SST gradient weakens moisture convergence over Northern China, which reduces summer monsoon precipitation (Figure 5a). This enhances drought potential

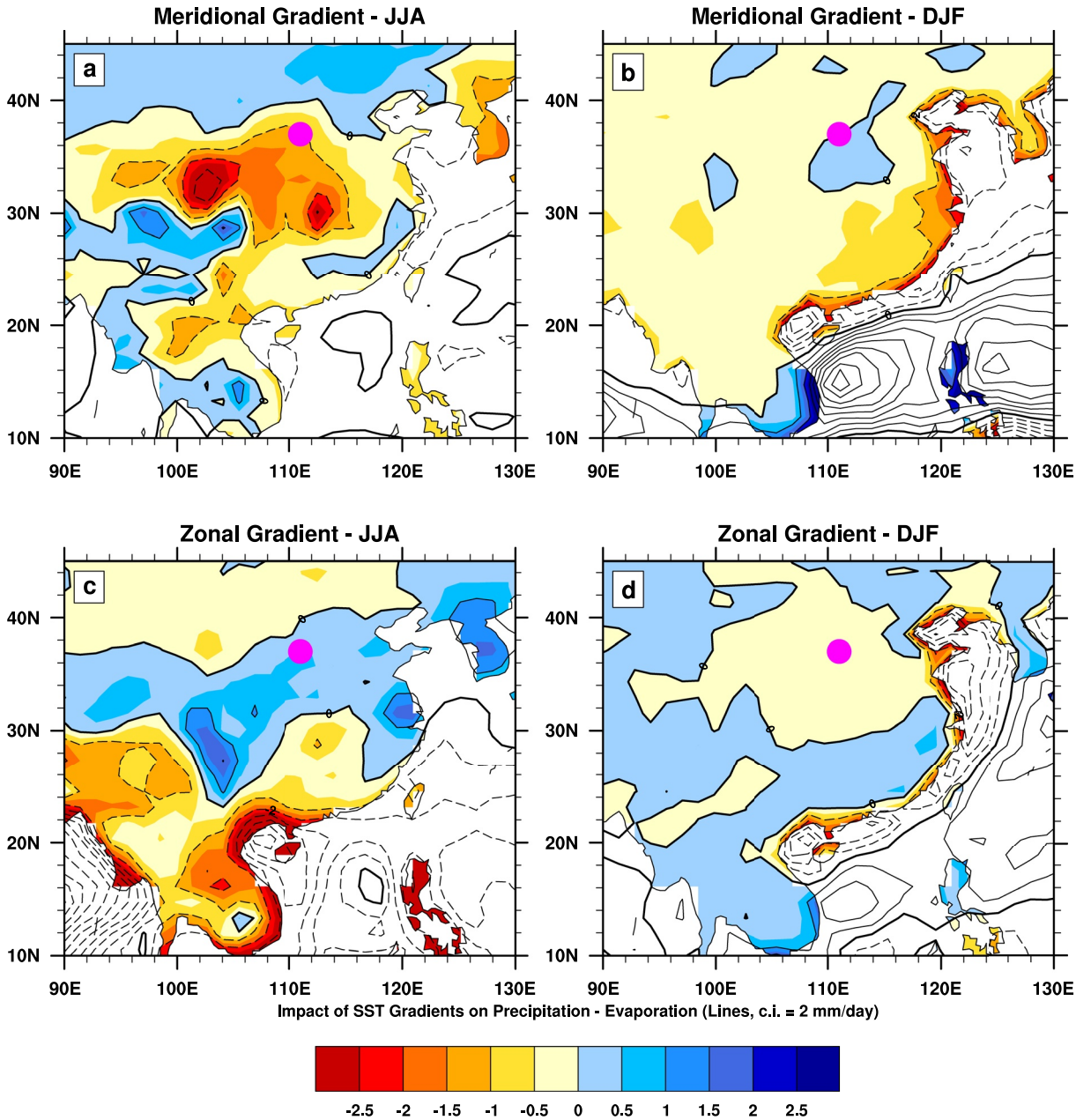

Figure 5. Impacts of the reduced zonal and meridional sea surface temperature gradients on P-E in an atmospheric general circulation model in panels (a and c) summer and (b and d) winter seasons. Yellow/red colors indicate more arid conditions. The magenta marker indicates the location of Shilou. Thin dashed and solid lines indicate negative and positive contours, respectively, and the zero contour is shown by thick solid lines.

in North China because its rainfall is largely governed by the Asian summer monsoon, with about 85% of the annual precipitation delivered between May and September by moisture-laden air masses sourced from the Pacific Ocean.

4. Discussion and Conclusion

We have reconstructed hydroclimate evolution on the CLP during the Pliocene Epoch based on GDGT distributions. The $R_{i/b}$ (and BIT) ratios are stable and low (high) during the late Pliocene, but they show sharp peaks during the early Pliocene, indicating extreme drought conditions during the latter time interval. These drought

conditions appear to be much more severe than arid conditions suggested by grain size and magnetic susceptibility as reported previously.

Combining data and modeling results we find that the reduced meridional SST gradient is the likely critical factor in the weakening of the East Asian monsoon precipitation over Northern China and in maintaining drought conditions over the CLP during the early Pliocene. Both coupled and atmosphere-only experiments strongly support the key role of the meridional SST gradient in controlling summer precipitation over the CLP and the surrounding regions of North China. The reduction of the meridional SST gradient weakens the East Asian summer monsoon precipitation over Northern China through the reduction of northward moisture transport from the ocean that is able to reach this region.

Overall, the effect of the reduced zonal SST gradient along the equator (mean El Niño-like conditions) may have also contributed to the enhanced aridity, but the link between P-E over the CLP and the zonal SST gradient is somewhat weaker. This is related to the fact that the zonal SST gradient reduction weakens CLP precipitation in winter, which is of less importance than monsoonal precipitation in summer. Finally, we hypothesize that the apparent ending of drought conditions over the CLP around 4 Ma may reflect a threshold behavior. Both zonal and meridional temperature gradients were weaker in the early Pliocene than in the mid-Pliocene. With the gradual increase of the SST gradients over this time interval, precipitation over North China was gradually increasing as well (Figure 4) until a sufficient threshold was reached, possibly triggering climate-vegetation feedbacks (Tierney et al., 2017).

Thus, our work provides new observational and modeling evidence for understanding the impacts of the zonal and especially meridional SST gradients on crucial teleconnection patterns and the hydrological cycle of the North Pacific region during the warm early Pliocene epoch and possibly in the future warmer world.

Data Availability Statement

The proxy data generate by this study are available at https://doi.org/10.5281/zenodo.6699975. The additional datasets cited in Figure 2 are available in these citation references: Fedorov et al., 2013; Liu et al., 2019; Wara et al., 2005; Pagani et al., 2010; LaRiviere et al., 2012; Lisiecki & Raymo, 2005. The climate model simulations with different meridional and zonal SST gradients have been archived in Zenodo: https://doi.org/10.5281/zenodo.6762450 and https://doi.org/10.5281/zenodo.6762717. The atmospheric GCM simulations to isolate the effects of zonal versus meridional SST gradients have been archived in Zenodo: https://doi.org/10.5281/zenodo.6760131. The code used to make the synthetic timeseries is available on GitHub (https://github.com/nburls/ZhengEtAl2022).

Acknowledgments
This work was supported by the National Natural Science Foundation of China Grants (41872031, 41372033, 41772027), the Key Scientific and Technological Team Project in Shaanxi Province, and funds from the State Key Laboratory of Loess and Quaternary Geology (SKLLQG1731). Additional support to A. V. Fedorov from the ARCHANGE project of the "Make our planet great again" program (ANR-18-MPGA-0001, France) is acknowledged. We thank two anonymous reviewers and the editor for their valuable comments.

References

An, Z. S., Huang, Y. S., Liu, W. G., Zhang, Q. L., Cao, Y. N., Qiang, X. K., et al. (2005). Multiple expansions of C_4 plant biomass in East Asia since 7 Ma coupled with strengthened monsoon circulation. *Geology*, *33*(9), 705–708. https://doi.org/10.1130/g21423.1

An, Z. S., Kutzbach, J. E., Prell, W. L., & Porter, S. C. (2001). Evolution of Asian monsoons and phased uplift of the Himalaya Tibetan plateau since Late Miocene times. *Nature*, *411*(6833), 62–66. https://doi.org/10.1038/35075035

Anwar, T., Kravchinsky, V. A., & Zhang, R. (2015). Magneto-and cyclostratigraphy in the red clay sequence: New age model and paleoclimatic implication for the eastern Chinese Loess Plateau. *Journal of Geophysical Research: Solid Earth*, *120*(10), 6758–6770. https://doi.org/10.1002/2015jb012132

Brierley, C. M., & Fedorov, A. V. (2010). The relative importance of meridional and zonal SST gradients for the onset of the Ice Ages and Pliocene-Pleistocene climate evolution. *Paleoceanography*, *25*(2), PA2214. https://doi.org/10.1029/2009pa001809

Burke, K. D., Williams, J. W., Chandler, M. A., Haywood, A. M., Lunt, D. J., & Otto- Bliesner, B. L. (2018). Pliocene and Eocene provide best analogs for near-future climates. *Proceedings of the National Academy of Sciences of the United States of America*, *115*(52), 13288–13293. https://doi.org/10.1073/pnas.1809600115

Burls, N. J., & Fedorov, A. V. (2014). What controls the mean East–West sea surface temperature gradient in the equatorial Pacific: The role of cloud albedo. *Journal of Climate*, *27*(7), 2757–2778. https://doi.org/10.1175/jcli-d-13-00255.1

Burls, N. J., & Fedorov, A. V. (2017). Wetter subtropics in a warmer world: Contrasting past and future hydrological cycles. *Proceedings of the National Academy of Sciences of the United States of America*, *114*(49), 12888–12893. https://doi.org/10.1073/pnas.1703421114

Dai, A. G., & Wigley, T. M. L. (2000). Global patterns of ENSO-induced precipitation. *Geophysical Research Letters*, *27*(9), 1283–1286. https://doi.org/10.1029/1999gl011140

Ding, Z. L., Yang, S. L., Hou, S. S., Wang, X., Chen, Z., & Liu, T. S. (2001). Magnetostratigraphy and sedimentology of the Jinchuan red clay section and correlation of the Tertiary eolian red clay sediments of the Chinese Loess Plateau. *Journal of Geophysical Research*, *106*(B4), 6399–6407. https://doi.org/10.1029/2000jb900445

Dirghangi, S. S., Pagani, M., Hren, M. T., & Tipple, B. J. (2013). Distribution of glycerol dialkyl glycerol tetraethers in soils from two environmental transects in the USA. *Organic Geochemistry*, *59*, 49–60. https://doi.org/10.1016/j.orggeochem.2013.03.009

Dowsett, H. J., Robinson, M. M., Haywood, A. M., Hill, D. J., Dolan, A. M., Stoll, D. K., et al. (2012). Assessing confidence in Pliocene sea surface temperatures to evaluate predictive models. *Nature Climate Change*, *2*(5), 365–371. https://doi.org/10.1038/nclimate1455

Fedorov, A. V., Brierley, C., & Emanuel, K. (2010). Tropical cyclones and permanent El Nino in the early Pliocene epoch. *Nature*, *463*(7284), 1066–1070. https://doi.org/10.1038/nature08831

Fedorov, A. V., Brierley, C. M., Lawrence, K. T., Liu, Z., Dekens, P. S., & Ravelo, A. C. (2013). Patterns and mechanisms of early Pliocene warmth. *Nature*, *496*(7443), 43–49. https://doi.org/10.1038/nature12003

Fedorov, A. V., Burls, N. J., Lawrence, K. T., & Peterson, L. C. (2015). Tightly linked zonal and meridional sea surface temperature gradients over the past five million years. *Nature Geoscience*, *8*(12), 975–980. https://doi.org/10.1038/ngeo2577

Feng, R., Bhattacharya, T., Otto-Bliesner, B. L., Brady, E. C., Haywood, A. M., Tindall, J. C., et al. (2022). Past terrestrial hydroclimate sensitivity controlled by Earth system feedbacks. *Nature Communications*, *13*(1), 1–11. https://doi.org/10.1038/s41467-022-28814-7

Ford, H. L., Ravelo, A. C., Dekens, P. S., LaRiviere, J. P., & Wara, M. W. (2015). The evolution of the equatorial thermocline and the early Pliocene El Padre mean state. *Geophysical Research Letters*, *42*(12), 4878–4887. https://doi.org/10.1002/2015gl064215

Foster, G., Royer, D., & Lunt, D. (2017). Future climate forcing potentially without precedent in the last 420 million years. *Nature Communications*, *8*(1), 14845. https://doi.org/10.1038/ncomms14845

Han, Z., Zhang, Q., Li, Q., Feng, R., Haywood, A. M., Tindall, J. C., et al. (2021). Evaluating the large-scale hydrological cycle response within the Pliocene Model Intercomparison Project Phase 2 (PlioMIP2) ensemble. *Climate of the Past*, *17*(6), 2537–2558. https://doi.org/10.5194/cp-17-2537-2021

Haug, G., Ganopolski, A., Sigman, D., Rosell-Mele, A., Swann, G., Tiedemann, R., et al. (2005). North Pacific seasonality and the glaciation of North America 2.7 million years ago. *Nature*, *433*(7028), 821–825. https://doi.org/10.1038/nature03332

Haywood, A. M., Hill, D. J., Dolan, A. M., Otto-Bliesner, B. L., Bragg, F., Chan, W. L., et al. (2013). Large-scale features of Pliocene climate: Results from the Pliocene Model Intercomparison Project. *Climate of the Past*, *9*(1), 191–209. https://doi.org/10.5194/cp-9-191-2013

Haywood, A. M., Tindall, J. C., Dowsett, H. J., Dolan, A. M., Foley, K. M., Hunter, S. J., et al. (2020). The Pliocene Model Intercomparison Project Phase 2: Large-scale climate features and climate sensitivity. *Climate of the Past*, *16*(6), 2095–2123. https://doi.org/10.5194/cp-16-2095-2020

Huang, R., & Wu, Y. (1989). The influence of ENSO on the summer climate change in China and its mechanism. *Advances in Atmospheric Sciences*, *6*(1), 21–32. https://doi.org/10.1007/bf02656915

LaRiviere, J., Ravelo, A. C., Crimmins, A., Dekens, P. S., Ford, H. L., Lyle, M., & Wara, M. W. (2012). Late Miocene decoupling of oceanic warmth and atmospheric carbon dioxide forcing. *Nature*, *486*(7401), 97–100. https://doi.org/10.1038/nature11200

Lisiecki, L. E., & Raymo, M. E. (2005). A Pliocene-Pleistocene stack of 57 globally distributed benthic $\delta^{18}O$ records. *Paleoceanography*, *20*(1), PA1003. https://doi.org/10.1029/2004pa001071

Liu, J. J., Tian, J., Liu, Z. H., Herbert, T. D., Fedorov, A. V., & Lyle, M. (2019). Eastern equatorial Pacific cold tongue evolution since the late Miocene linked to extratropical climate. *Science Advances*, *5*(4), eaau6060. https://doi.org/10.1126/sciadv.aau6060

Lu, H. X., Liu, W. G., Yang, H., Wang, H. Y., Liu, Z. H., Leng, Q., et al. (2019). 800-kyr land temperature variations modulated by vegetation changes on Chinese Loess Plateau. *Nature Communications*, *10*(1), 1–10. https://doi.org/10.1038/s41467-019-09978-1

Lu, J., Yang, H., Griffiths, M. L., Burls, N. J., Xiao, G., Yang, J., et al. (2021). Asian monsoon evolution linked to Pacific temperature gradients since the Late Miocene. *Earth and Planetary Science Letters*, *563*, 116882. https://doi.org/10.1016/j.epsl.2021.116882

Nie, J. S., Stevens, T., Song, Y. G., King, J. W., Zhang, R., Ji, S., et al. (2014). Pacific freshening drives Pliocene cooling and Asian monsoon intensification. *Scientific Reports*, *4*(1), 5474. https://doi.org/10.1038/srep05474

Pagani, M., Liu, Z., LaRiviere, J., & Ravelo, A. (2010). High Earth-system climate sensitivity determined from Pliocene carbon dioxide concentrations. *Nature Geoscience*, *3*(1), 27–30. https://doi.org/10.1038/ngeo724

Peterse, F., Martínez-García, A., Zhou, B., Beets, C. J., Prins, M. A., Zheng, H. B., & Eglinton, T. I. (2014). Molecular records of continental air temperature and monsoon precipitation variability in East Asia spanning the past 130,000 years. *Quaternary Science Reviews*, *83*, 76–82. https://doi.org/10.1016/j.quascirev.2013.11.001

Qin, J., Zhang, R., Kravchinsky, V. A., Valet, J.-P., Sagnotti, L., Li, J., et al. (2022). 1.2 Myr band of Earth-Mars obliquity modulation on the evolution of cold late Miocene to warm early Pliocene climate. *Journal of Geophysical Research: Solid Earth*, *127*(4), e2022JB024131. https://doi.org/10.1029/2022JB024131

Robinson, M. M., Dowsett, H. J., & Chandler, M. A. (2008). Pliocene role in assessing future climate impacts. *Eos*, *89*(49), 501–502. https://doi.org/10.1029/2008eo490001

Shankle, M. G., Burls, N. J., Fedorov, A. V., Thomas, M. D., Liu, W., Penman, D. E., et al. (2021). Pliocene decoupling of equatorial Pacific temperature and pH gradients. *Nature*, *598*(7881), 457–461. https://doi.org/10.1038/s41586-021-03884-7

Sun, Y. B., An, Z. S., Clemens, S. C., Bloemendal, J., & Vandenberghe, J. (2010). Seven million years of wind and precipitation variability on the Chinese Loess Plateau. *Earth and Planetary Science Letters*, *297*(3–4), 525–535. https://doi.org/10.1016/j.epsl.2010.07.004

Tang, C. Y., Yang, H., Pancost, R. D., Griffiths, M. L., Xiao, G., Dang, X., & Xie, S. (2017). Tropical and high latitude forcing of enhanced megadroughts in Northern China during the last four terminations. *Earth and Planetary Science Letters*, *479*, 98–107. https://doi.org/10.1016/j.epsl.2017.09.012

Tierney, J. E., Haywood, A. M., Feng, R., Bhattacharya, T., & Otto-Bliesner, B. L. (2019). Pliocene warmth consistent with greenhouse gas forcing. *Geophysical Research Letters*, *46*(15), 9136–9144. https://doi.org/10.1029/2019gl083802

Tierney, J. E., Pausata, F. S. R., & de Menocal, P. B. (2017). Rainfall regimes of the Green Sahara. *Science Advances*, *3*(1), e1601503. https://doi.org/10.1126/sciadv.1601503

Wang, H., Liu, W., Zhang, C. L., Liu, Z., & He, Y. (2013). Branched and isoprenoid tetraether (BIT) index traces water content along two marsh-soil transects surrounding Lake Qinghai: Implications for paleo-humidity variation. *Organic Geochemistry*, *59*, 5–81. https://doi.org/10.1016/j.orggeochem.2013.03.011

Wang, H. L., Lu, X., Zhao, L., Zhang, H., Lei, F., & Wang, Y. (2019). Asian monsoon rainfall variation during the Pliocene forced by global temperature change. *Nature Communications*, *10*(1), 5272. https://doi.org/10.1038/s41467-019-13338-4

Wang, Y., Lu, H., Wang, K., Wang, Y., Li, Y., Clemens, S., et al. (2020). Combined high- and low-latitude forcing of East Asian monsoon precipitation variability in the Pliocene warm period. *Science Advances*, *6*(46), eabc2414. https://doi.org/10.1126/sciadv.abc2414

Wara, M. W., Ravelo, A. C., & Delaney, M. L. (2005). Permanent El Niño-like conditions during the Pliocene warm period. *Science*, *309*(5735), 758–761. https://doi.org/10.1126/science.1112596

Weijers, J. W. H., Schouten, S., Hopmans, E. C., Geenevasen, J. A. J., David, O. R. P., Coleman, J. M., et al. (2006). Membrane lipids of mesophilic anaerobic bacteria thriving in peats have typical archaeal traits. *Environmental Microbiology*, *8*(4), 648–657. https://doi.org/10.1111/j.1462-2920.2005.00941.x

White, S. M., & Ravelo, A. C. (2020). Dampened El Niño in the early Pliocene warm period. *Geophysical Research Letters*, *47*(4), e2019GL085504. https://doi.org/10.1029/2019gl085504

Xie, S., Pansost, R. D., Chen, L., Evershed, R. P., Yang, H., Zhang, K., et al. (2012). Microbial lipid records of highly alkaline deposits and enhanced aridity associated with significant uplift of the Tibetan Plateau in the Late Miocene. *Geology*, *40*(4), 291–294. https://doi.org/10.1130/g32570.1

Yang, H., Pancost, R. D., Dang, X., Zhou, X., Evershed, R. P., Xiao, G., et al. (2014). Correlations between microbial tetraether lipids and environmental variables in Chinese soils: Optimizing the paleo-reconstructions in semi-arid and arid regions. *Geochimica et Cosmochimica Acta*, *126*, 49–69. https://doi.org/10.1016/j.gca.2013.10.041